Aerospace Science and Technology 118 (2021) 107000

Contents lists available at ScienceDirect

Aerospace Science and Technology

www.elsevier.com/locate/aescte

Twin-fuselage configuration for improving fuel efficiency of passenger aircraft

Yiyuan Ma *, Ali Elham

Technische Universität Braunschweig, Braunschweig, 38108, Germany

ARTICLE INFO

Article history:
Received 8 February 2021
Received in revised form 6 July 2021
Accepted 28 July 2021
Available online 8 August 2021
Communicated by Cummings Russell

Keywords:
Twin-fuselage configuration
Conceptual design
Wing mass estimation
Design space exploration
Multidisciplinary design optimization

ABSTRACT

The requirements of increasing air traffic volume while enhancing its sustainability for the next generation of air transportation demand a step change in aircraft performance, for which the development and technology escalation of ultra-high aspect ratio wings configurations is one key enabling strategy. However, compared with conventional aircraft, the ultra-high aspect ratio wings structure bears higher loads, which poses challenges to aircraft configuration design and related technologies. This paper describes the twin-fuselage (TF) concept as one of the promising configurations adopting ultra-high aspect ratio wings. A methodology of conceptual design and analysis framework for TF transport aircraft is developed by improving and integrating several methods and tools. A medium-range TF transport aircraft is designed, and a sensitivity analysis is carried out to explore the design space, and multidisciplinary design optimization is used to optimize the configuration of the TF transport aircraft. The results show a significant advantage of TF configuration over the conventional cantilever configuration, which presents reductions of 29.33% and 33.60% in the fuel consumption and maximum takeoff weight, respectively.

1. Introduction

Due to the rapid growth of air transportation demand, more and more attention is focused on the impact of air transportation on the environment and climate [1]. Challenging goals outlined in Flightpath 2050 by the European Commission (EC) advocate a 75% CO_2-emissions reduction, a 90% NO_x-emissions reduction, and a 65% perceived noise reduction with respect to the capabilities of conventional aircraft of the year 2000 [2]. These ambitious goals lead to the development of novel aircraft concepts and technologies to make future transport aircraft more environmentally-friendly.

There are a large number of ongoing research projects related to novel transport aircraft concepts to improve the fuel economy and reduce emissions for the next-generation transport aircraft [3]. Boeing is conducting a research project, Subsonic Ultra Green Aircraft Research (SUGAR), funded by NASA, which is about the comprehensive investigation on the strut-braced wing (SBW) aircraft configuration with high aspect ratio wings [4]. Massachusetts Institute of Technology (MIT) and Aurora Flight Sciences are developing D8.x aircraft which feature a “double-bubble” cross-section fuselage as well as high aspect ratio wings [5]. Researchers from Technische Universität Braunschweig are investigating the influence of game-changing technologies on the energy efficiency of future transport aircraft under the program of the German Cluster of Excellence Sustainable and Energy Efficient Aviation (SE2A) [6], in which several unconventional aircraft configurations are being studied, such as forward-swept wing concept for a medium-range mission and blended wing body (BWB) concept for a long-range mission.

Almost all of the aforementioned aircraft are designed with a high aspect ratio wing concept because increasing the wing aspect ratio can effectively reduce the induced drag, which accounts for 40% of the total aircraft drag of an A320-like transport aircraft [7]. However, as the wing aspect ratio increases, the shear force and bending moment caused by the aerodynamic load will increase from the wingtip to the wing root, which will lead to a large warpage deformation of the wingtip, and the wing will be easy to fatigue and break [8].

Twin-fuselage (TF) aircraft configuration is one of the promising concepts to reduce the shear force and bending moment on the wing, allowing a further increase of wing aspect ratio [9]. However, there has been little research on TF passenger aircraft recently, possibly due to the challenges it poses to airport infrastructure (e.g., runway width and terminal access). Moreover, performing re-

* Corresponding author.
E-mail address: yiyuan.ma@tu-braunschweig.de (Y. Ma).

https://doi.org/10.1016/j.ast.2021.107000

Symbols and abbreviations

b	wing span, m
C_D	drag coefficient
C_L	lift coefficient
c	chord, m
d	diameter, m
E_T	effective airfoil thickness coefficient
g	gravitational acceleration, m/s^2
H	height, m
k	factor
L/D	lift-to-drag ratio
l	length, m
M	mass, kg
Mo	spanwise distribution of bending moment, N·m
Ma	Mach number
m	relative mass (mass divided by aircraft mass)
n	overload factor
P	spanwise distribution of specific thickness ratio
Q	spanwise distribution of shear force, N
q	spanwise distribution of load, N
S	area, m^2
T	absolute airfoil thickness, m
V	volume, m^3
y	spanwise relative coordinate
σ_u	ultimate direct stress, N/m^2
σ_{us}	ultimate shear stress, N/m^2
κ	scaling factor for folding-wing mechanisms
Λ	wing sweep, deg
λ	outboard wing taper ratio
ρ	density of structural material, kg/m^3

Subscripts

a	aerodynamic load
ail	ailerons
cg	center of gravity
cr	cruise
e	engine
f	fuselage
fu	fuel
fold	folding
flap	flaps
M	bending moment
mac	mean aerodynamic chord
man	manufacturing
Q	shear stress
r	root of the wing
rib	ribs
s	wing structure
sk	load-free wing skin
sl	service life
sum	sum
TO	takeoff
tw	twist moment
y	y-coordinate
z	z-coordinate

search on TF transport aircraft is not simple because there is not much experience or a database for this kind of aircraft.

This paper describes a preliminary investigation of the TF configuration's potentials for improving passenger aircraft fuel efficiency. Section 2 introduces the benefits and research progress of the TF configuration. Section 3 presents the development of the design and analysis framework for TF aircraft. Section 4 presents a case study of a medium-range TF transport aircraft, which demonstrates the application of the design and analysis method established in Section 3. Section 5 showcases the design space exploration and multidisciplinary design optimization (MDO) for the TF aircraft. Section 6 presents a comparative study of the TF configuration's characteristics. Finally, the findings of this work are summarized in Section 7.

2. Twin-fuselage configuration

The high aspect ratio wing concept can improve aircraft aerodynamic efficiency and fuel efficiency and reduce emissions [10]. However, increasing the wing aspect ratio for conventional configurations will often lead to an increase of wing bending moment and shear force, which increases the design requirements for the strength and stiffness of the wing structure. For this reason, TF aircraft configuration appeared, which reduces wing bending moment and allows a lighter wing structure by replacing the large mass of the centrally positioned fuselage by two masses positioned outboard [11], as shown in Fig. 1.

Besides the weight reduction in the wing structure, a decrease in fuselage weight can be expected for TF configuration as well. As the skin thickness of a pressure cabin is proportional to its volume, if the TF aircraft cabins are designed to have the same total floor area as conventional aircraft, the two skins together of TF aircraft will have a weight equal to that of the conventional aircraft divided by $\sqrt{2}$ [13]. Furthermore, TF configuration has an

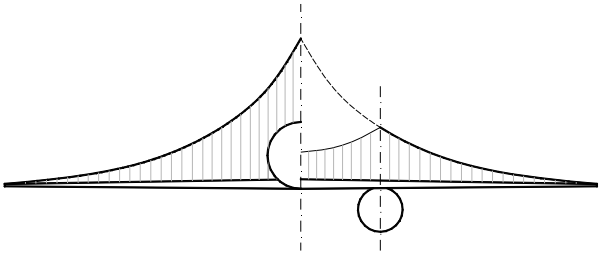

Fig. 1. Wing bending moment comparison [12].

ideal location for the main landing gear, although an additional nose landing gear is required [14]. For the TF configuration, the external fairings are not required for the main landing gear, and the strut length and mechanisms of the main landing gear can be reduced and simplified, which provides benefits for weight and drag reduction.

However, there are also some challenges when designing a TF aircraft, such as the adverse aerodynamic interaction between the wings with two fuselages and the challenges posed to airport infrastructure. Besides, the off-centerline located fuselages cause a different mass spanwise distribution compared to conventional aircraft, which will change moments of inertia of TF aircraft and influence the roll and yaw motion [11].

Although the TF concept has not been studied in detail for transonic passenger aircraft, this concept has already been successfully implemented in large transonic airplanes and unmanned aerial vehicles, proving the maturity of related technologies. Scaled Composites developed a twin-fuselage, twin-empennage, 6-engine aircraft Stratolaunch carrier aircraft for an air-launch space access system, which is the largest all-composite aircraft ever built [15]. Virgin Galactic developed a large, four-engine, twin-fuselage jet aircraft WhiteKnightTwo to serve as the launcher of the sub-orbital

SpaceShipTwo [16]. Langelaan et al. [17] developed a two-seat, twin-fuselage, self-launching sailplane Taurus G4 for the Green Flight Challenge 2011 organized by Comparative Aircraft Flight Efficiency Foundation and NASA and won the first prize. The German Aerospace Center (DLR) has successfully developed and flown a twin-fuselage, 4-seat aircraft, HY4, powered by a hydrogen fuel cell system [18]. Ma et al. [19] developed a distributed electric propulsion (DEP), twin-fuselage, unmanned aerial vehicle (UAV) as an experimental platform for DEP technology and TF configuration. Carithers et al. [20] connected two small fixed-wing aircraft to be a TF aircraft and performed a flight test to study the control system for the TF aircraft. Gao et al. [21] designed and tested the performance characteristics of a twin-fuselage, solar-powered UAV.

As for the research on the TF passenger aircraft, NASA conducted several research projects on the TF passenger aircraft and TF transport aircraft decades ago. For example, Lockheed and NASA conducted the conceptual design and wind tunnel experiments for a large cargo TF aircraft to replace the Lockheed C-5A and the Boeing 747 transport aircraft in the future [14] and carried out the simulator study of the flight characteristics of the TF transport aircraft during approach and landing [22]. Subsequently, NASA carried out an in-flight investigation of a 250-PAX TF passenger aircraft [23]. Besides, Udin et al. [24] derived a formula to estimate the wing structural mass of TF aircraft. De Jong et al. [11] improved the wing weight estimation method developed by Udin et al. [25] for the H-cabin configuration, TF passenger aircraft. However, no TF passenger aircraft has been developed previously, probably due to airport infrastructure constraints (e.g., runway width and terminal access) and the complexity of TF aircraft development (e.g., flight dynamics and airworthiness certification). But with the emergence and maturity of many advanced technologies in recent years, such as folding wingtips and composites wings, it is necessary to study again the possibility of applying the TF configuration to the next-generation air transportation. Recently, there have been some studies on the TF passenger aircraft. Chiesa et al. [9] presented a TF aircraft preliminary case study designed with similar parameter values to the reference conventional aircraft. Vedernikov et al. [12] described the disadvantages of the traditional single-fuselage scheme and analyzed the TF aircraft scheme through a case study design based on the prototype of A320. Russian Central Aerohydrodynamic Institute (TsAGI) [25] conducted wind tunnel experiments for a TF transport airplane. However, these studies on the TF transport aircraft neither introduce the complete conceptual design method of TF aircraft nor show the detailed design process of the design cases, which is challenging to be used as a reference in the next-generation TF passenger aircraft design.

3. Conceptual design method

3.1. Novel technologies for the next-generation transport aircraft

For the next-generation transport aircraft, a large number of research on advanced technologies is being conducted in the fields of aerodynamics, control, materials, and so on, which are expected to be applied to the next-generation transport aircraft to reduce emissions. One of the goals of this research is to investigate the influence and the potential of combining advanced technologies with the unconventional configuration to reduce emissions. The novel technologies used in this research are briefly introduced in the following.

3.1.1. Hybrid laminar flow control (HLFC)

Natural laminar flow (NLF) is a promising approach to significantly reduce viscous wing drag for aircraft [7]. However, it is difficult to maintain a large NLF area on the wing for large aircraft with high wing sweep angles. Therefore, HLFC systems need to be integrated into the wing and tails to delay flow transition [26]. The HLFC concept integrates NLF by active boundary layer flow control, which has the potential to reduce the overall aircraft drag by up to 50% [7].

3.1.2. Load alleviation

Aircraft structures need to be sized for worst-case operating conditions, which is reflected by the load factors. Load alleviation introduces various technologies to reduce the loads experienced by the aircraft. The reduction of maximum loads enables the design of a lighter wing and fuselage for lower limit load factors, improving fuel efficiency.

A load alleviation research carried out by the DLR [27] showed that the wing mass of a large long-range passenger aircraft could be reduced by about 45% if the maximum positive load factor of $+2.5$ g was reduced to $+1.5$ g by using advanced load alleviation techniques. Such radical load reductions make it necessary to drastically redistribute the spanwise lift distribution during maneuvers by flow actuation [6]. Besides, extremely rapid systems (viscoelastic damping design) are required to mitigate the effects of an atmospheric gust to dump wing lift. Furthermore, aeroelastic tailoring and advanced systems for flight control are also required [28].

3.1.3. Advanced materials and structure

Over the past decades, composites have gradually replaced traditional metallic material in aircraft structures. For the structural materials of next-generation transport aircraft, tow steering is a novel method of variable stiffness composite design, which can result in a 15% reduction in structural weight compared to conventional composite structure [29]. Moreover, thin ply materials could be used in composite fiber reinforced polymers (CFRP) structures to reduce the inter-laminate stresses due to finite ply thickness, resulting in the potential of wing weight reductions of about 10% [6].

These advanced technologies need to be considered and assumed at the initial sizing stage to investigate the potential effects of these technologies on the overall efficiency and performance characteristics of TF aircraft.

3.2. Conceptual design environment

In this research design of a TF passenger aircraft equipped with the abovementioned technologies is considered to investigate the potentials of this configuration to improve the fuel efficiency of aircraft. Besides, comprehensive sensitivity analysis and design optimization are presented to guide future development on TF aircraft design.

Several tools were used for the conceptual design and analysis of TF aircraft. An initial aircraft sizing tool PyInit [28], an in-house tool developed by the authors, was used for the initial aircraft sizing and performance analysis. OpenVSP [30] was used for the aircraft geometric modeling, and the open-source aircraft design environment Stanford University Aerospace Vehicle Environment (SUAVE) [31] was used for the multi-fidelity analysis of the weight breakdown, aerodynamics, flight performance, and missions.

PyInit integrated various semi-empirical and physics-based formulations for constraint diagram, aerodynamics, stability and control, propulsion, tail sizing, and flight performance [28]. Initial aircraft sizing in PyInit starts from analyzing constraints according to the top-level requirements. Then the wing loading and thrust-to-weight ratio could be determined, and the components, including the wing, fuselage, and empennage of the aircraft, can be sized. Finally, various analysis containing aerodynamics, stability and control, and performance characteristics could be selected and performed for the sized aircraft.

However, as introduced, PyInit is an initial sizing tool to obtain the initial aircraft concept and geometric components such as the wing aspect ratio, sweep, and tail volume ratios, but the weight and mission segments convergent iterations are not included. Therefore, after the initial sizing using PyInit, the geometry of the sized aircraft is imported into SUAVE for the iterative calculations to modify the aircraft geometry and weights to meet the mission requirements.

The latest version of SUAVE already has the modules of analyzing some unconventional aircraft configurations, such as BWB aircraft, solar-powered UAV, electric vertical takeoff and landing (eVTOL) aircraft, etc. However, SUAVE currently has no analysis modules for SBW and TF configurations, which have great potential to be utilized in the ultra-high aspect ratio wings design. Therefore, SUAVE has been improved in this research, adding an analysis module for TF aircraft, including wing weight estimation method, parasite drag estimation method, and the influence of advanced technologies such as HLFC, load alleviation, and advanced materials and structures. The detailed method and design process are introduced in the following.

3.3. Structural mass estimation

The most remarkable difference between TF and conventional aircraft in the design method is the wing mass estimation due to the significantly different loads spanwise distribution on the wing. While for the mass estimation of other components, including fuselage, empennage, and engine, conventional methods could be utilized.

3.3.1. Wing mass estimation method

For the unconventional wing configurations, the finite element method (FEM) has great adaptability and accuracy through creating beam elements and shell elements and applying exacted loads to the model to calculate the wing mass. However, FEM requires more information and development time, outweighing its benefits at the conceptual design stage. Therefore, this section focuses on establishing a wing mass estimation method for TF aircraft that balances efficiency and accuracy and applies to the conceptual design stage with limited information available.

The traditional wing mass estimation method is developed based on the assumption that the bending moment of wings on both sides of the fuselage is balanced at the fuselage position (i.e., the aircraft's centerline). The comparison of the wing bending moment spanwise distribution of TF and conventional aircraft is shown in Fig. 1. If the mass of the TF aircraft fuselages is simply treated as the way of treating the engine mass load in the traditional semi-empirical method (i.e., adding two outboard concentrated loads representing the mass of fuselages), the bending moment distribution of the inboard wing section will be incorrect. Therefore, the wing mass estimation method for TF aircraft needs to be developed according to its specific load spanwise distribution.

A semi-analytical wing mass estimation method for TF aircraft developed by Udin [25] is used in this research. In this method, the relative wing structural mass is calculated by integrating the wing spanwise mass distribution (including wing structure mass, fuel mass, and concentrated mass such as the engines) with the aerodynamic load spanwise distribution. Each fuselage is assumed as a concentrated load, including the mass of the fuselage structure, empennage structure, payload, crew, avionics system, etc., i.e., all that is not located on the wing. The relative mass of the wing structure is given by

$$m_s = k_{sl} k_{tw} k_{man} \left(m_M + m_Q\right) + m_{rib} + m_{ail} + m_{sk} + m_{flap} \tag{1}$$

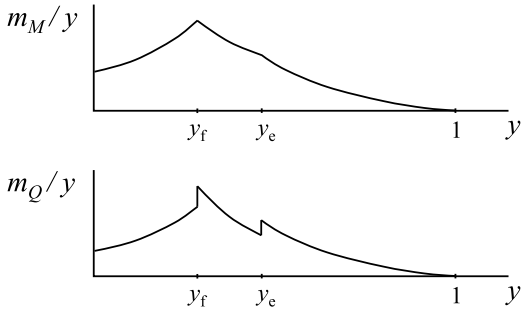

Fig. 2. Spanwise distribution of relative wing mass [25].

where the values and formula of the service life factor k_{sl}, the twist moment factor k_{tw}, and the manufacturing factor k_{man} can be referred to Ref. [25]. The m_M and m_Q are the estimated relative structural mass counteracting the wing bending moment and shear force, which can be expressed as

$$m_M = 2\frac{\rho n_z g}{\sigma_u T_r}\frac{b^2}{4} E_T \int_0^1 \frac{Mo_{sum}}{P(y)\cos\Lambda} dy \tag{2}$$

$$m_Q = \frac{\rho n_z g}{\sigma_{us}}\frac{b}{2}\int_0^1 \frac{Q_{sum}}{\cos\Lambda} dy \tag{3}$$

where the M_{sum} and Q_{sum} represent the total reduced bending moment and total reduced shear force caused by aerodynamic loads, wing structural mass, fuel mass, and concentrated mass. The reduced bending moment and reduced shear force can be obtained by integration, as

$$Mo(y) = \int_y^1 Q(y)\, dy \tag{4}$$

$$Q(y) = \int_y^1 q_a(y)\, dy \tag{5}$$

The spanwise aerodynamic distribution load q_a can be simplified by linear or quadratic approximation at the conceptual design stage. More accurate wing structural mass estimation results can be obtained by introducing high-precision aerodynamic data from computational fluid dynamics (CFD) calculations. If a linear approximation is used, the spanwise distribution of aerodynamic load for the inboard wing section ($0 < y < y_f$) can be written as

$$q_a = \frac{2}{y_f(1-\lambda)+\lambda+1} \tag{6}$$

And for the outboard wing ($y_f < y < 1$):

$$q_a = 2\frac{[(1-y)/(1-y_f)](1-\lambda)+\lambda}{y_f(1-\lambda)+\lambda+1} \tag{7}$$

The spanwise distribution of relative wing mass needed to carry bending moment and shear force is shown in Fig. 2. The detailed derivation process and integral calculations of the above formula can be found in Ref. [25].

The wing secondary structures of TF aircraft are similar to those of conventional aircraft. Therefore, existing semi-empirical methods given by Udin [25] and Torenbeek [13] could be used for the mass estimation of the secondary structures, including ailerons, leading-edge flaps, trailing edge flaps, etc.

Table 1
Validation of the wing mass estimation methodology.

Parameter	Estimated	Actual value [32]	Error, %
m_s	0.1132	0.1185	−4.47
Wing mass, kg	100863	105555	−4.45

For validation, the large TF cargo aircraft designed by Lockheed and NASA was selected, and the required data was extracted from Moore [32]. This aircraft is a very large cargo aircraft with 1990s technology, designed to replace the Lockheed C-5A and the Boeing 747 in the future transport aircraft market [14]. The comparison and error analysis of the wing mass calculated using the presented method and the data from Ref. [32] are tabulated in Table 1. The wing mass estimation error is less than 5%, proving the presented wing mass estimation method gives acceptable results.

One of the main difficulties in developing ultra-high aspect ratio wing aircraft is the airport gate-box limit on the wingspan. For example, generally, medium-range passenger aircraft operate at ICAO Code C airport with a gate-box limit of 36 m (118 ft). Therefore, the ultra-high aspect ratio wing aircraft needs to be designed with foldable wings, increasing its mass. An estimation method for wing mass penalty of the folding-wing mechanisms can be found in Ref. [33], which is given by

$$\frac{m_{\text{fold}}}{M_{\text{TO}}} = \kappa \frac{Q_s}{M_{\text{TO}}} \tag{8}$$

where κ is a scaling factor, which can be taken as 0.07 for the Boeing 777 aircraft [33]. Q_s/M_{TO} can be written as

$$\frac{Q_s}{M_{\text{TO}}} = \frac{1}{2}\left(1 - \frac{2}{\pi} y_{\text{fold}} \sqrt{1 - y_{\text{fold}}^2} - \frac{2}{\pi} \sin^{-1} y_{\text{fold}}\right) \tag{9}$$

3.3.2. Other components mass estimation method

Other TF aircraft components such as fuselage, empennage, and engine are very similar to conventional aircraft. Therefore, existing semi-empirical structural mass estimation methods developed for conventional aircraft could be used for the mass estimation of other components of TF aircraft.

Flight Optimization System (FLOPS) was developed by NASA to design and synthesize new aircraft configurations at the conceptual design stage and evaluate the impacts of advanced technologies [34]. FLOPS has been extensively used and verified in the field of aircraft design [35,36]. In this research, FLOPS was utilized and improved to consider the influence of HLFC and advanced materials for the future advanced passenger aircraft, and then used for the mass estimation of other components of TF aircraft.

3.4. Fuselage sizing

The fuselage sizing process for TF aircraft is divided into three parts: initial sizing, interior arrangement, and cargo capacity check. Their process and relationship are shown in Fig. 3.

3.4.1. Initial sizing

The most significant feature of the TF concept is the unique fuselage configuration. However, there is currently no fuselage sizing method for TF aircraft that has been published. At present, the fuselage of conventional aircraft can be taken as the reference for the fuselage sizing of a TF aircraft, and a sizing criterion is necessary for this method. For TF passenger aircraft, the same total floor area as that of the conventional aircraft can be used as the sizing criteria to ensure that the number of passenger seats remains unchanged. Subsequently, the sized fuselage geometry needs to be coordinated with the cabin interior arrangement and cargo containers. The same total volume of the fuselage can be taken as the sizing criterion for cargo aircraft.

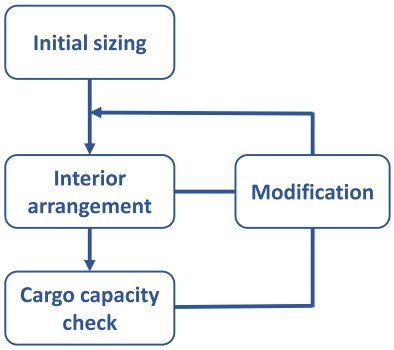

Fig. 3. Fuselage sizing process.

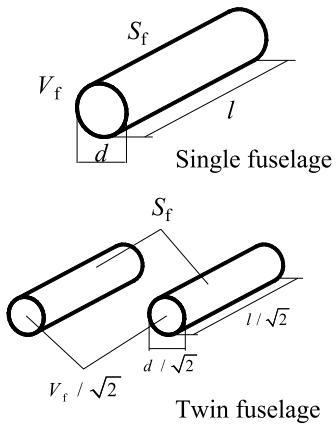

Fig. 4. Parameters of the two configurations with the same floor area [13].

As shown in Fig. 4, according to the sizing criteria proposed above, the length and equivalent diameter of each fuselage of TF aircraft are $l/\sqrt{2}$ and $d/\sqrt{2}$, respectively, and the two skins together have an equal wetted area to that of the single-fuselage configuration.

Besides, the main landing gear span of commercial aircraft is also limited. For the aircraft operating at ICAO Code C airport, the main landing gear span should not exceed 9 meters, which means that the distance between the two fuselages of this kind of TF aircraft should not exceed 9 meters.

3.4.2. Interior arrangement

Since both the length and width are reduced to keep the fuselage fitness ratio constant, the number of the seats in the row should not be simply divided by 2 when determining the interior arrangement of each fuselage of TF aircraft. For example, if the reference single-fuselage aircraft has a 6-abreast seating arrangement, a 4-abreast seating arrangement for each TF aircraft fuselage is recommended. It needs to be checked in detail whether all of the cabin's parameters meet the requirements refer to the Certification Specification 25 (CS 25) [37] as well as the suggestions in Refs. [38,39], including the aisle width, aisle height, seat width, seat pitch, and so on. If some parameters of the fuselage cabin do not meet the requirements, the fuselage geometry needs to be modified within a reasonable range.

3.4.3. Cargo capacity

A negative consequence of the TF concept is that the total cargo hold volume of the two fuselages is reduced relative to the single-fuselage layout, as the total fuselage volume of TF aircraft is equal to that of the single-fuselage layout divided by $\sqrt{2}$ as shown in Fig. 4. Therefore, it is necessary to check whether the cargo hold capacity meets the requirements. For example, the luggage weight

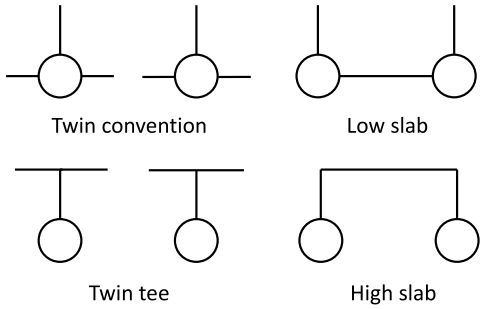

Fig. 5. Empennage configuration alternatives.

for each passenger is not less than 23 kg. If the result is unacceptable, the twin-fuselage cross-sections will have to be modified to match the required cargo hold capacity.

3.5. Empennage configuration

There are several alternative empennage configurations for TF aircraft, as shown in Fig. 5. These layouts can be generally divided into two categories: high-horizontal tail layout and low-horizontal tail layout.

As described in the fuselage sizing section, the fuselage length of TF aircraft is shorter than that of conventional aircraft, resulting in a shorter tail moment arm, larger tail area, and heavier tail structural weight. The high-horizontal tail concept can increase the tail arm, which is beneficial to reduce the structural weight of the horizontal tail. Besides, due to the endplate effect of the high-horizontal tail, the vertical tail area of this configuration can also be reduced. Also, the stability and control effectiveness of the low-horizontal tail will be influenced by the downwash of the wing. Therefore, in general, the high-horizontal tail layout has more advantages for TF aircraft.

The horizontal slab tails have a higher aspect ratio, resulting in a higher lift coefficient. For this reason, the volume ratio of the horizontal tail can be reduced, thereby making the horizontal tail lighter.

3.6. Landing gear design

The landing gear design of the TF concept is also different from that of conventional configuration. The TF aircraft has one nose landing gear and one main landing gear located on each fuselage centerline, laterally spaced at a distance between the two fuselages. This distance can meet the required ground operation roll stability, which is usually provided by extending the length of the main landing gear strut of conventional aircraft laterally as much as possible, which increases the weight of the main landing gear.

The nose landing gear and main landing gear retract forward or backward (free-fall) and stowed underneath the cabin floor. Therefore, external fairings are not required for the main landing gear. Furthermore, the doors of the nose and main landing gear can be simply designed to operate mechanically as a function of the gear extends and retract motion. Hence, an independent system is not required.

In summary, even if the TF aircraft has one more nose landing gear, the landing gear of TF aircraft will be simpler and lighter than that of conventional aircraft. For very large cargo aircraft, this weight reduction can even reach 30% [14].

3.7. Conceptual design framework

Since the aircraft configuration undergoes considerable changes at each iteration in the initial design stage, validated engineering methods for aerodynamic analysis can be used. Therefore, a vortex lattice method (VLM) and correlations available in SUAVE are used to predict lift and drag for TF aircraft. Fig. 6 shows the flowchart of the conceptual design and analysis process for TF aircraft established in this research.

As introduced, currently SUAVE does not have an analysis module for TF aircraft. Therefore, in this study, the wing weight estimation method of TF aircraft was added to the structural weight analysis module of SUAVE. Additional fuselage, vertical tail, and nose landing gear were defined in the main analysis script for weight and aerodynamic analysis. Moreover, the influence factors due to the advanced technologies, including HLFC, advanced materials and structure, and load alleviation, were added to the aerodynamic and weight analysis modules of each component.

The aforementioned largo cargo TF aircraft designed by Lockheed and NASA was used to verify the accuracy of the TF aircraft analysis method established in SUAVE. The geometry, mission profile, etc. of the large cargo TF aircraft were input into SUAVE, and the results of the relative errors calculated by SUAVE for the weight and aerodynamic characteristics of the largo cargo TF aircraft are given in Table 2.

Table 2
Validation of the TF aircraft analysis method established in SUAVE.

Parameter	SUAVE	Reference value [32]	Error, %
MTOW, kg	863885	891128	−3.06
OEW, kg	314174	335250	−6.29
Fuel Weight, kg	199732	205900	−2.99
C_L	0.485	0.509	−4.72
C_D	0.0226	0.0220	2.64
L/D	21.48	23.14	−7.17

Table 3
Assumptions of advanced technologies.

Technology	Assumption
HLFC	55% of the wing and empennages area
Load alleviation	Ultimate load factors are +1.5 g and −0.5 g
Advanced materials & structures	20% structural weight reduction

4. Case study: a medium-range TF transport aircraft

The conceptual design of a medium-range TF transport aircraft is conducted to investigate the potentials of combining the TF configuration with novel airframe technologies for reducing fuel consumption of passenger aircraft. Besides, this test case aircraft is used for a series of sensitivity analyses, providing further guidelines for TF configuration design.

A medium-range transport aircraft comparable to the A320neo is considered here, with a harmonic range of 3400 nautical miles and 150 passengers (two-class). The entry into service (EIS) time of this aircraft is assumed to be the year 2040. The assumptions on the influence of advanced technologies for this aircraft are given in Table 3, regarding Refs. [40,41]. Similar to A320neo, the cruise speed of this aircraft is set to $Ma_{cr} = 0.78$ at a cruise altitude of 33,000 ft, and the service ceiling is set at 38,500 ft. Furthermore, a diversion range of 200 nm is required, with a 3% contingency fuel and 10-minute hold at 1,500 ft considering the EIS time is 2040 (currently requirements are 5% contingency fuel, 200 nm diversion range, and 30-minute hold) [40]. Besides, this medium-range transport aircraft will operate at the ICAO Code C airport category, so the wingspan cannot exceed 118 ft, and the main landing gear span cannot exceed 29.5 ft. This aircraft is designed to comply with CS-25 [37]. These top-level requirements on the conceptual design are collected in Table 4, and the mission profile is shown in Fig. 7.

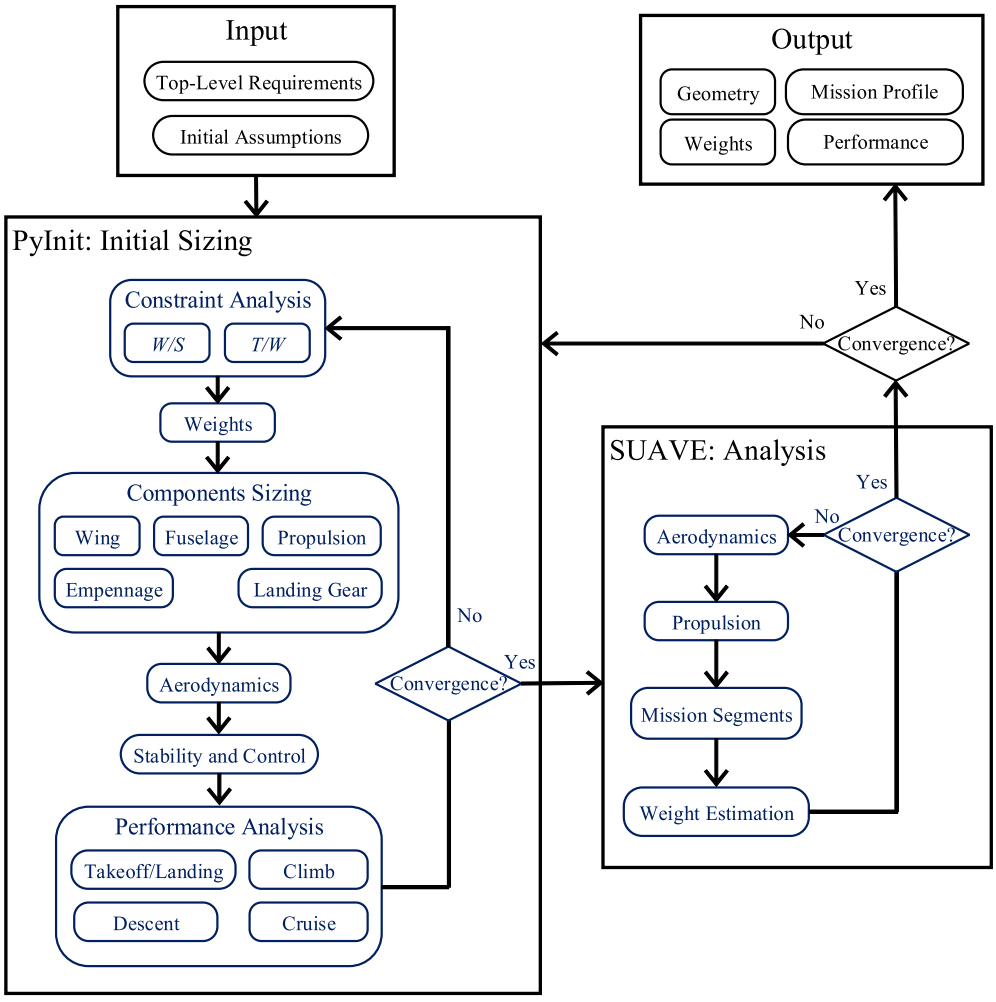

Fig. 6. Flowchart of the conceptual design and analysis process.

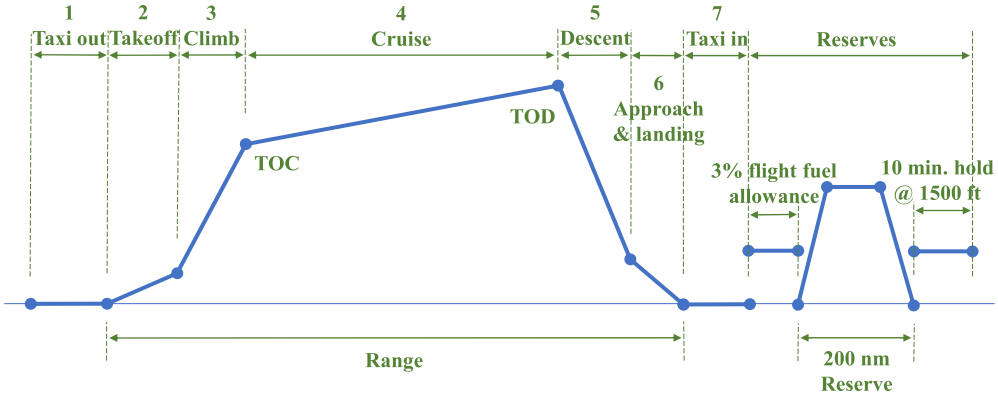

Fig. 7. Mission profile of the medium-range transport aircraft.

4.1. Initial sizing

The initial aircraft sizing with all the advanced technologies assumed in Table 3 was performed to determine the geometric and performance characteristics of the future TF aircraft. The aircraft initial sizing tool PyInit and the multi-fidelity aircraft design environment SUAVE, modified in this research project, introduced in Section 3, were used for the initial sizing and performance analysis of the medium-range TF transport aircraft.

As shown in Fig. 8, the thrust-to-weight ratio and wing loading of the medium-range TF aircraft are selected as 0.282 and 86.3 lb/ft^3 respectively, which were determined according to the top-level requirements and the design specifications derived from existing medium-range transport aircraft, such as A320neo. Besides, for comparison, the values of A320 [42] and several similar advanced medium-range transport aircraft, including SUGAR [40], SE2A-MR [6], D8.5 [43], and SD8.5 [43], are also shown in Fig. 8.

Table 4
Top-level requirements.

Requirement	Value
Cruise Mach number	0.78
Cruise altitude, ft	33,000
Service ceiling, ft	38,500
Range, nm	3400
Passengers	150
Approach speed, kt	136
Diversion range, nm	200
Contingency fuel	3%
Diversion hold, min	10
Gate-box limit, ft	118
Main landing gear span, ft	29.5

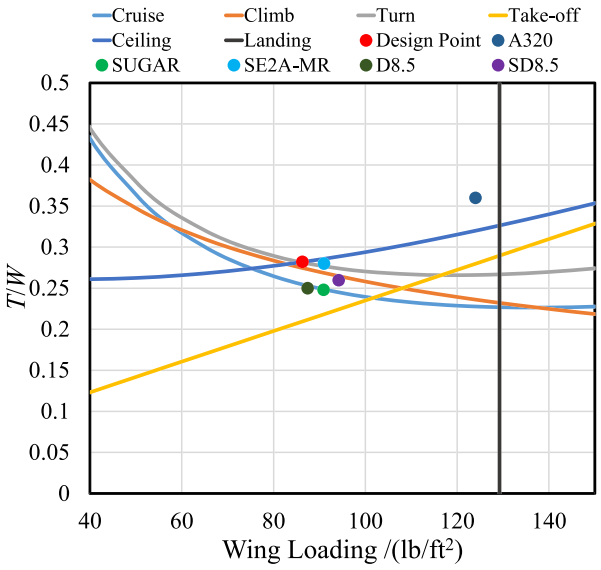

Fig. 8. Constraint diagram. (For interpretation of the colors in the figure(s), the reader is referred to the web version of this article.)

The initial aircraft configuration and the three-view dimensions of the aircraft are shown in Fig. 9 and 10, and the design parameters used in the initial sizing are listed in Table 5. The aircraft has a high-wing configuration with two wing-mounted high bypass ratio turbofan engines. Since the wingspan is limited to 118 ft, a folding wing need to be designed, with the folding position at 118/2 ft of the half-span. The supercritical airfoils NASA SC(2)-0412 and NASA SC(2)-0410 were selected as the airfoils of the wing root and wingtip, respectively. Moreover, the high-slab empennage configuration was used, and the horizontal tail was designed as a forward-swept configuration. The reasons for this choice are that, on the one hand, this concept could increase the horizontal tail moment arm to reduce the horizontal tail area, and on the other hand, this design would reduce the wave drag of the horizontal tail (compared to a zero swept tail). The scissors plot of the TF aircraft generated by PyInit is shown in Fig. 11, which was used for the aircraft's initial tail sizing. This aircraft has a CG travel of about 38% MAC, and the static margin is 9%. Besides, the supercritical NASA SC(2)-0010 was selected as the empennage airfoil.

The fuselage of the A320neo was taken as the reference for the TF transport aircraft fuselage sizing. The length of the A320neo fuselage is 123.27 ft, the width is 12.96 ft, and the height is 13.58 ft [42]. The fuselage sizing method for TF aircraft introduced in Section 3 was used to ensure the same cabin floor area is achieved. The dimensions of the sized fuselage are given in Table 5.

After the initial sizing of the fuselage geometry, the interior arrangement needs to be carried out. For the two-class cabin layout, the design requirement for the total number of passengers

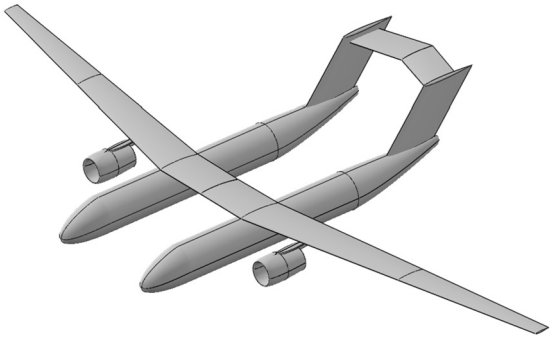

Fig. 9. The configuration of the medium-range TF transport aircraft.

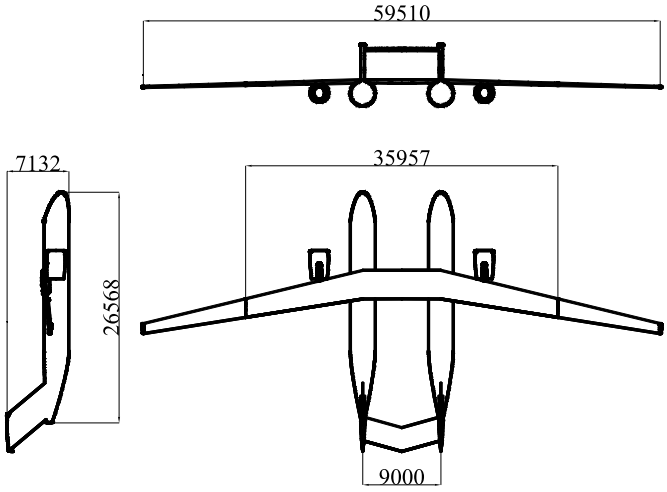

Fig. 10. Three-view dimensions of the TF aircraft.

Table 5
Design parameter values.

Component	Parameter	Value
Wing	Aspect ratio	25.0
	Taper ratio	0.35
	Reference area, ft^2	1461.08
	Span, ft	191.12
	Outboard wing sweep (0.25c), deg	12.5
	Root chord, ft	10.51
	Tip chord, ft	3.69
Fuselage	Number	2
	Length, ft	87.17
	Height, ft	9.60
	Width, ft	9.16
	Equivalent diameter, ft	9.38
Horizontal tail	Aspect ratio	3.49
	Taper ratio	1.0
	Span, ft	19.53
	Quarter-chord sweep, deg	−15.5
Vertical tail	Aspect ratio	1.0
	Taper ratio	1.0
	Span, ft	13.77
	Quarter-chord sweep, deg	40.0

was taken as 150, which is consistent with that of the A320neo [42]. The economy class of the TF aircraft has a 4-abreast seating arrangement for each fuselage. In contrast, the A320neo has a 6-abreast seating arrangement. For this TF transport aircraft, the nose of one fuselage was designed as the cockpit, while the nose of the other fuselage was arranged with two super-first-class seats with the best view, as shown in Fig. 12. This arrangement can make full

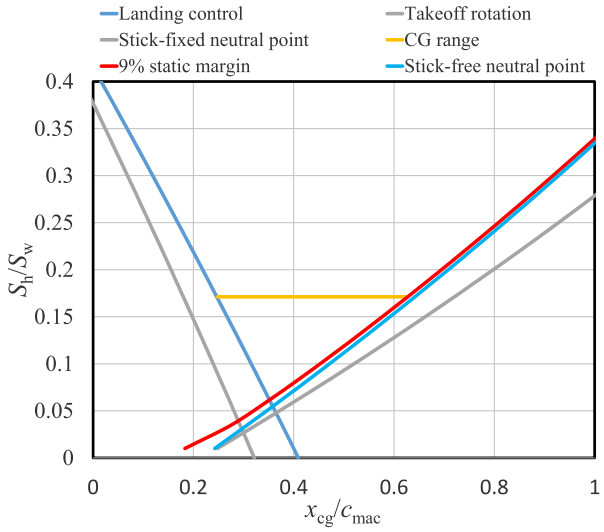

Fig. 11. Scissors plot for tail sizing of the TF aircraft.

Table 6
Cargo capacity.

Parameter	Value
Total cargo volume, m^3	25.69
Loading efficiency	0.85
Average cargo density, kg/m^3	160
Total cargo capacity, kg	3494.27
Cargo capacity per passenger, kg	23.30

use of the space in the fuselage and bring more profits for airlines. The cross-section of the fuselage is shown in Fig. 13. All parameters meet the cabin design requirements, such as the minimum passenger aisle width should not be less than 15 in [37], and the aisle height should be greater than 76 in [38].

The cargo capacity of the TF transport aircraft and the ability of the aircraft to accommodate the standard cargo containers used today need to be examined. Several existing standard types of cargo containers are available, such as LD1, LD2, and LD3, and 95% of the cargo containers are LD3 type, which is used by A320 series aircraft [44]. However, the LD3 container cannot directly fit into the TF aircraft fuselage. Refer to the D8 series aircraft design [43], a candidate container denoted here as LDx could be developed and put into operation in the EIS timeframe of 2040 to allow the TF aircraft to incorporate cargo. As shown in Table 6, each passenger's cargo capacity is 23.30 kg, which meets the passenger luggage design requirement [39].

4.2. Performance analysis

The modified SUAVE, improved for the future TF transport aircraft, was used to converge the weights and ensure the satisfaction of the required flight missions. The TF aircraft configuration obtained during the initial sizing process using PyInit was input into SUAVE for iterative calculations until the gross weight and missions converge. The analysis results are given in Table 7 and Figs. 14–17.

It should be noted that according to the proposed wing mass estimation method, the wing box of the medium-range TF aircraft is 1299.77 kg, accounting for 38.55% of the total wing mass, while the wing secondary structures mass is 2071.88 kg. Elham et al. [45] developed a regression between the ratio of the wing box weight to the wing total weight and the aircraft takeoff weight, which is given by

$$W_{\text{wingbox}}/W_{\text{wing}} = 0.1571 M_{\text{TO}}^{0.2505} \quad (10)$$

Table 7
Weight breakdown summary of the medium-range TF aircraft.

Group	Weight, kg
Max. takeoff weight	56510
Max. zero fuel weight	43469
Fuel weight	13041
Empty weight	29249
Empty weight breakdown	**Weight, kg**
Wing	3842
Fuselages	5241
Propulsion	3584
Nacelles	484
Landing gear	1936
Horizontal tail	754
Vertical tail	826
Paint	410
Systems	12172

Table 8
Selected design parameters.

Category	Parameter
Technology	Laminar flow area
Geometry	Fuselage fitness ratio
	Fuselage spanwise location
	Aspect ratio
	Taper ratio
	Wing sweep
Operation	Cruise Mach number
	Cruise altitude

According to Eq. (10), the ratio of the wing box weight to the wing total weight for a conventional aircraft with the same M_{TO} as the medium-range TF aircraft should be 43.16%. Therefore, it can be seen that the ratio of the wing box weight to the wing total weight of the TF aircraft is slightly smaller than that of the conventional aircraft, due to the larger rolling moment of the TF aircraft, which requires larger ailerons and high-lift systems. Besides, it is worth noting that according to the method presented in Sec. 3.3.1 for estimating the wing mass penalty due to the folding mechanisms, the wing mass penalty of the medium-range TF aircraft is 0.9483% of M_{TO}, i.e., 13.95% of the wing mass.

The HLFC technology was applied to the wing and empennage of the TF transport aircraft. To analyze the impact of HLFC technology on aircraft aerodynamic characteristics, especially drag characteristics, the comparison of parasite drag breakdown with or without HLFC is shown in Fig. 18.

The comparison between the medium-range TF transport aircraft and A320neo will be shown in the subsequent section, together with the optimized configuration.

5. Sensitivity analysis and optimization

5.1. Design space exploration

Even though the designed medium-range TF aircraft with assumed technologies demonstrated substantial performance improvements compared to conventional aircraft, we still do not know enough about TF aircraft characteristics. Therefore, sensitivity analysis (i.e., design space exploration) was performed for the TF aircraft to study how the design parameters influence the aircraft characteristics. The selected design parameters for the analysis are listed in Table 8.

The sizing procedure of the design space exploration for each configuration was performed for the same mission profile and used the similar methods described in Section 3 to ensure the sized configuration meets all top-level requirements. Fig. 18 shows

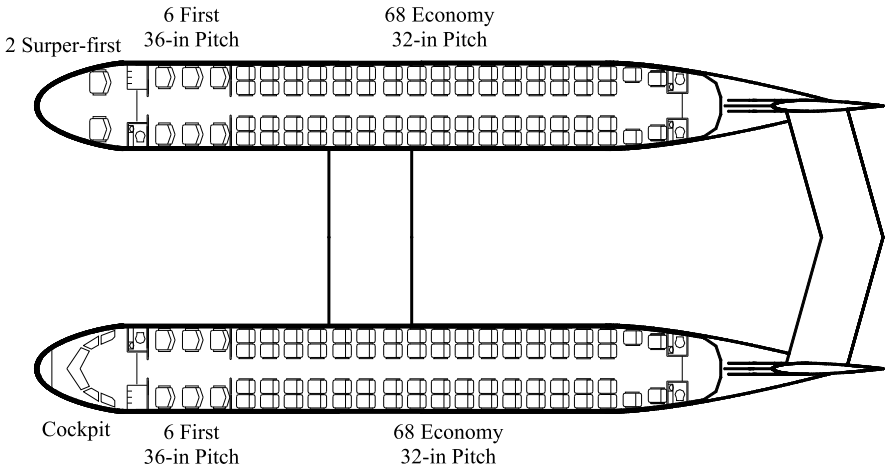

Fig. 12. The interior arrangement of the TF aircraft.

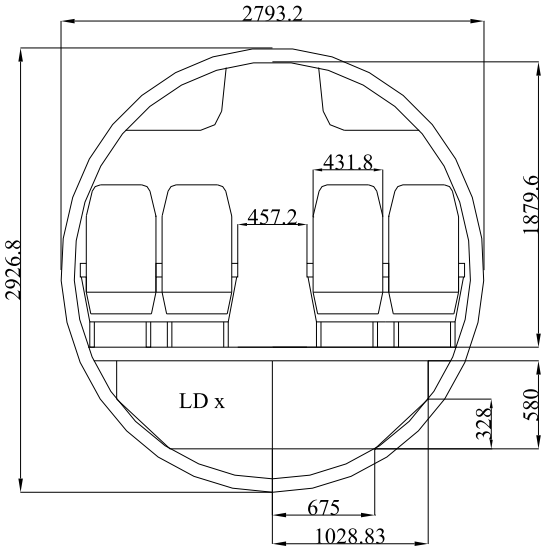

Fig. 13. Fuselage cross-section of the TF aircraft.

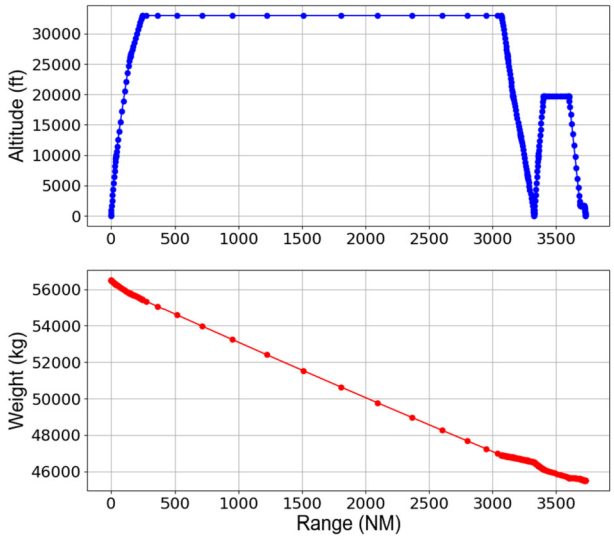

Fig. 14. Mission performance of the TF aircraft.

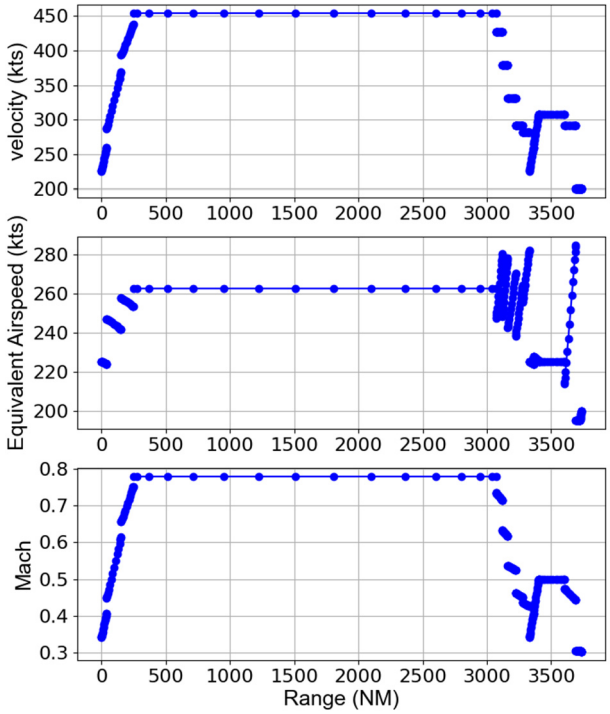

Fig. 15. Velocity profiles of the TF aircraft.

the design space exploration results. The vertical dashed line in each figure indicates the baseline of the studied parameter used in the initial configuration sizing, and the design space exploration changes the value of the parameter based on the baseline.

As shown in Fig. 19, the fuel weight and MTOW decrease rapidly with increased laminar flow area on the wing and empennage, showing a linear trend. When the HLFC technology is developed to be able to maintain 80% of the laminar flow area on the wing and empennage, compared with the current technical level (assuming 20% natural laminar flow), the fuel weight and MTOW of the TF aircraft will be reduced by 42.06% and 14.91%, respectively. The sharp reduction in fuel weight is mainly due to the significant reduction in the required thrust as the laminar flow area increases. The obtained results show that HLFC technology development is very significant for weight reduction, emission reduction, and economic improvement for the next-generation transport aircraft.

In the initial sizing of the TF aircraft, the fuselage fitness ratio was set to be the same as that of A320neo, resulting in the

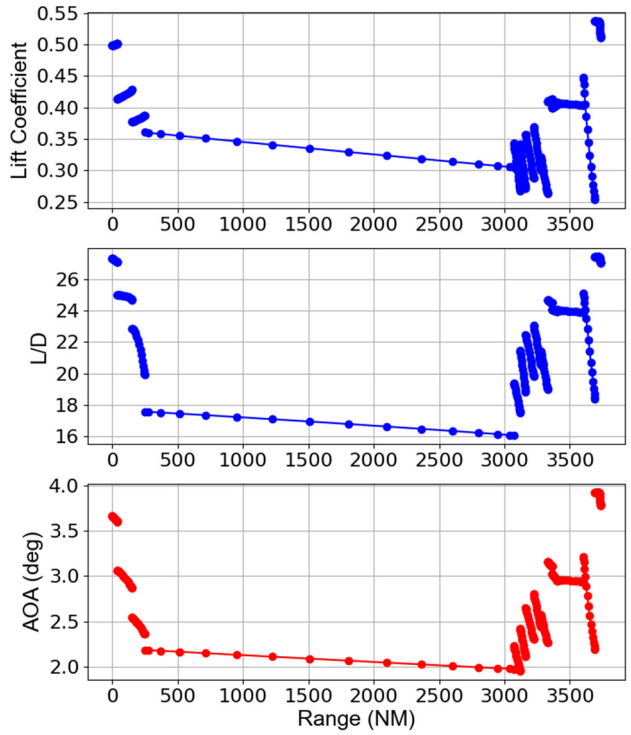

Fig. 16. Aerodynamic performance of the TF aircraft.

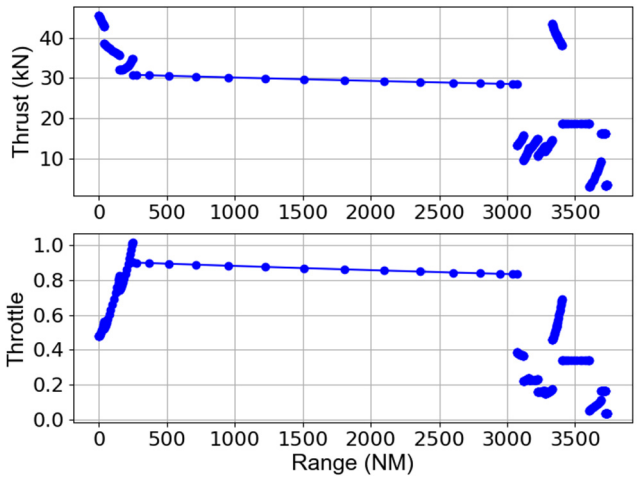

Fig. 17. Thrust and throttle settings of the TF aircraft.

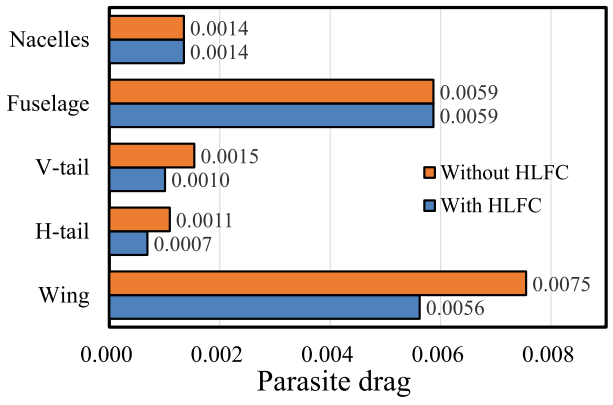

Fig. 18. Parasite drag breakdown comparison.

Table 9
Groups and values of multi-parameter sensitivity analysis.

Group	Parameter	Min. value	Max. value	Baseline value
1	Laminar flow area	0.4	0.8	0.55
	Max. load factor	1.5	2.5	1.5
2	Cruise Mach number	0.68	0.8	0.78
	Cruise altitude, ft	32000	40000	33000
3	Cruise Mach number	0.68	0.8	0.78
	Wing sweep, deg	5.0	40.0	12.5
4	Aspect ratio	20.0	30.0	25.0
	Taper ratio	0.3	0.6	0.35

fuselage length of the TF aircraft is smaller than that of A320neo, which means the tail area of the TF aircraft will be larger. The effect of the fitness ratio of the TF aircraft fuselage on the performance characteristics was studied in this research. As shown in Fig. 19, the fuel weight and MTOW of the TF aircraft is approximately exponentially related to the fuselage fitness ratio. This is not only due to the influence of the fuselage itself but also due to the change of the tail areas. However, as aforementioned, it is necessary to coordinate with the cabin interior arrangement when determining the fuselage fitness ratio.

The variation trends of the fuel weight and MTOW with the selected design parameters are similar, except for the aspect ratio. The fuel weight is approximately quadratically related to the aspect ratio. Within limits, the fuel weight decreases significantly with the increase of aspect ratio, while the MTOW shows an exponential increase trend, which is mainly due to the structural weight of the TF aircraft, especially the wing structural weight, increases with the rise of the aspect ratio. However, the fuel weight does not always decrease with the increase of the aspect ratio. When the aspect ratio increases to a particular value (around 27), the penalty caused by the increase of structural weight will exceed the aerodynamic benefits, resulting in increased fuel weight instead of decreasing.

Design space exploration results show that the sensitivities of fuel weight and MTOW of the TF aircraft to design parameters are different. The values of some design parameters of the baseline configuration are not optimal, indicating the performance of the initially designed TF aircraft could be improved.

As aircraft engineers well know, aircraft is a highly coupled complex system with multiple disciplines and various parameters, which means that the design parameters will have a coupling influence on aircraft performance. Therefore, the multi-parameter sensitivity analysis was performed to further explore the design space of the TF transport aircraft. As listed in Table 9, two related parameters were divided into a group, and a total of four groups were analyzed.

To improve the efficiency, the design of experiments (DOE) approach was used to sample the design space, and Kriging surrogate models [46] was used to approximate the design space. The DOE method of Latin Hypercube Sampling (LHS) was used to generate ten sets of data for each group, of which eight sets were used for the Kriging surrogate models training by using an open-source Matlab toolbox DACE [47], and two sets were used for the validation of the trained surrogate models. Fig. 20 shows the normalized DOE samples used for the analysis and surrogate models training. Then, the configurations corresponding to the two sets of data used for validation were analyzed using the trained Kriging models and SUAVE, respectively, and the errors of the results predicted by Kriging models relative to that calculated by SUAVE were analyzed. According to the results presented in Table 10, the fuel weight and takeoff weight were estimated by the Kriging models with acceptable accuracy (less than 5% error).

Fuel weight is the most concerned parameter of next-generation passenger aircraft as it is closely related to the direct operating

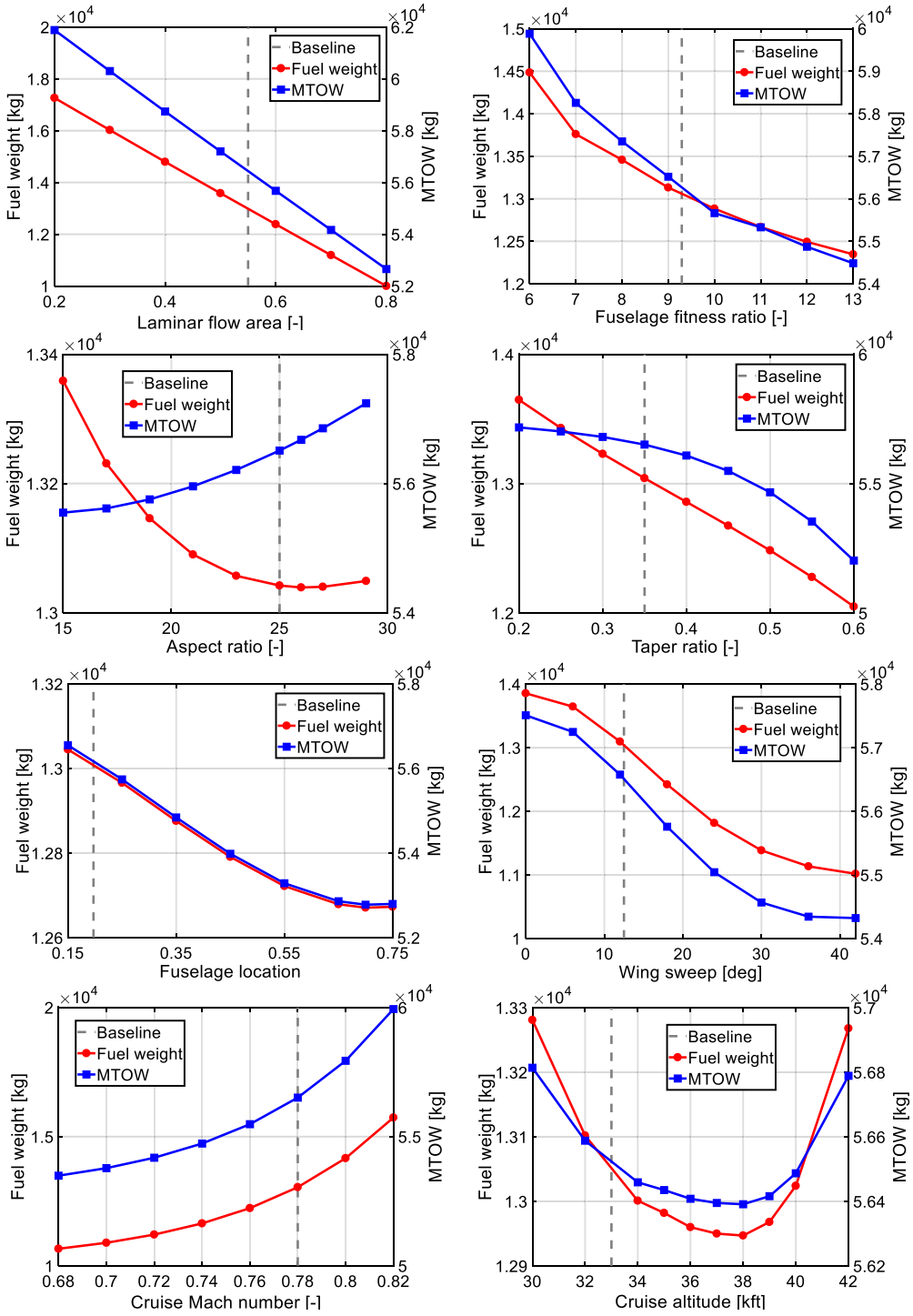

Fig. 19. Design space exploration of the selected parameters.

Table 10
Accuracy validation of the trained Kriging models.

Group	Configuration	Relative error, %	
		Fuel weight	Gross weight
1	1	−4.85	−1.16
	2	−0.44	0.03
2	1	4.67	1.31
	2	0.65	0.12
3	1	2.30	0.61
	2	−1.96	−0.54
4	1	−1.25	0.27
	2	−0.16	0.07

cost (DOC) and emissions. Multi-parameter sensitivity analysis of the fuel weight to the design parameters listed in Table 9 was performed, and the approximation of the design space by the Kriging models is shown in Fig. 21. The eight black dots in each figure represent the data used to train the Kriging models, and the two red dots represent the data used for the validation.

Firstly, because the two technology parameters of limit load factor and laminar flow area are not very tightly coupled, the minimum fuel weight can be obtained at the minimum limit load factor and maximum laminar flow area. When the cruise Mach number

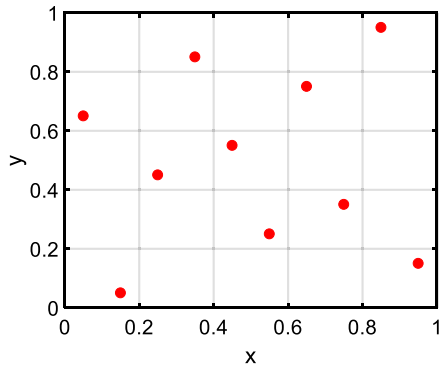

Fig. 20. LHS samples.

is low, the fuel weight first decreases and then increases with the increase of flight altitude, which is consistent with the results of single parameter sensitivity analysis in Fig. 19, while when the cruise Mach number is high (more than 0.78), the fuel weight will continue to decrease as the flight altitude increases. It is worth noting that when the wing sweep is different, the sensitivity of fuel weight to cruise speed is different, and the difference is very significant. For example, when the wing sweep angle is 0 degrees, the fuel weight increases exponentially with the increase of cruise Mach number due to the wave drag. However, as the wing sweep increases, the sensitivity of fuel weight to cruise Mach number will decrease significantly.

5.2. Multidisciplinary design optimization

Base on surrogate models, MDO was performed for the TF aircraft to find the optimal configuration satisfying all constraints, i.e., surrogate-based optimization. A widely used gradient-free genetic algorithm (GA) [48] with a high global optimization probability was used to avoid falling into a local optimum solution.

The MDO problem can be described as a search process mathematically using a set of design variables minimizing a specific objective function that represents the design goal. This search process was conducted considering numerous design constraints.

Several goals can be considered for the design optimization of an aircraft, such as the minimum takeoff weight, minimum fuel weight/emissions, and maximum lift-to-drag ratio [49], of which the minimum fuel weight goal emphasizes lower DOC and correlates to lower emissions, which is essential for the next-generation transport aircraft. Thus, the minimum fuel objective function was used for the MDO problem. Even though this goal does not involve the initial manufacturing cost of the aircraft, with the increasing fuel prices nowadays and the imminence of environmental issues, this objective function will be the most appropriate one.

Design variables of the TF transport aircraft contain the geometric and operational design parameters, including aspect ratio, wing sweep (quarter-chord of the outboard wing), taper ratio, cruise Mach number, and cruise altitude. The values ranges of these design variables were taken to be the same as those given in Table 9, but the upper bound of the wing leading edge sweep was set to 17 degrees because the laminar flow on the wing will be hard to keep if the wing sweep is large [40].

The design constraints considered in this MDO study composed of the aforementioned bounds of design variables, the mission profile shown in Fig. 7, and the top-level requirements listed in Table 4.

The MDO framework consists of several analysis modules. As shown in Fig. 22, the MDO framework contains three iteration loops: the MTOW convergence loop, the surrogate models loop, and the optimizer loop. The MTOW convergence loop finds the MTOW for a given configuration in SUAVE with the constraints of the mission profile and top-level requirements, and this loop includes the analysis modules of aerodynamic, propulsion system, mission segments, and weight estimation.

Firstly, the LHS method was used to generate 20 sets of design variables as input for SUAVE analysis to calculate the respective characteristics, including fuel weight, MTOW, and lift-to-drag ratio. The analysis results and the design variables were used to train the Kriging models and validate their accuracy. If the accuracy of the trained Kriging models meets the requirements, input them to the

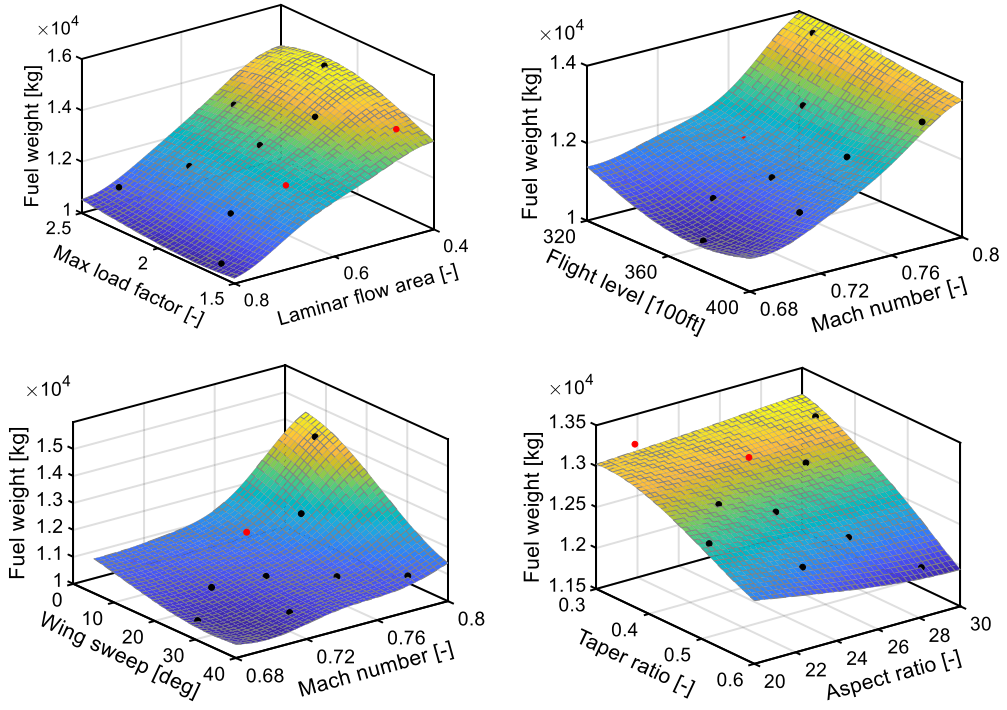

Fig. 21. Multi-parameter sensitivity analysis.

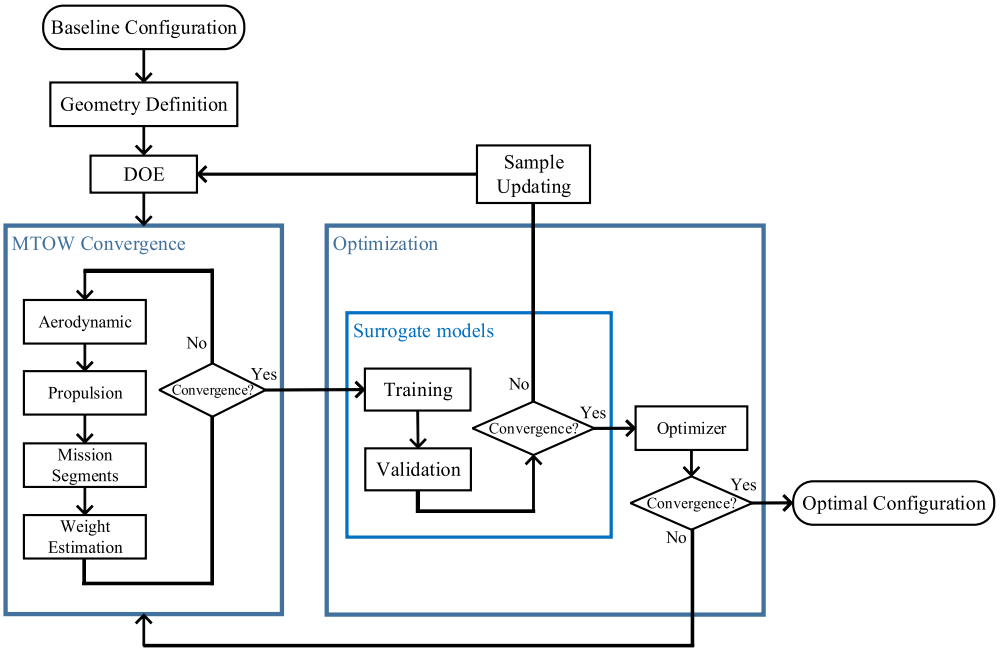

Fig. 22. MDO framework.

Table 11
The optimal configuration and validation.

	Design variables					Outputs		
	AR	λ	Λ, deg	Ma_{cr}	H_{cr}, kft	M_{fu}, kg	M_{TO}, kg	L/D
Optimization	27.872	0.490	16.994	0.7103	35.62	10337.0	52465.0	23.337
SUAVE	27.872	0.490	16.994	0.7103	35.62	10388.0	52459.0	23.527
Error, %	–	–	–	–	–	−0.49	0.01	−0.81

Table 12
Relative error analysis of MDO solutions for cross-validation.

Configuration	A	B	C	D	E
M_f	−3.71%	0.51%	−0.24%	0.28%	−0.21%
M_{TO}	−0.83%	0.10%	−0.39%	−0.20%	0.03%

optimizer using GA to search for the optimum solution of the minimum fuel objective function. Finally, the optimal configuration will be analyzed by SUAVE for validation. The optimum solution of the TF aircraft MDO problem is given in Table 11. The optimal configuration aspect ratio is 27.872, which is very close to the minimum value in the sensitivity analysis result of fuel weight to aspect ratio shown in Fig. 19.

Besides, five representative configurations (A, B, C, D, and E in Table 12) in the feasible solution sets of the MDO results were selected to cross-validate the surrogate models used in the optimization. The relative error analysis results of the five configurations are listed in Table 12, proving that the established MDO framework has good accuracy for the TF aircraft design optimization problem.

The geometric comparison between the baseline configuration, the optimal configuration, and the A320neo is shown in Fig. 23, and the weight characteristics comparison is listed in Table 13. For the optimal configuration, the reduction of the fuel weight is more than 20% compared to that of the baseline configuration, while the reduction of the maximum takeoff weight and operation empty weight is relatively low, which is less than 10%. This is mainly because the aerodynamic efficiency of the TF aircraft has been significantly improved during optimization, which will directly lead to the reduction of fuel weight. Moreover, with the same top-level requirements and mission profile, compared to A320neo, the operation empty weight reduction of the TF aircraft is greater than that of the maximum takeoff weight and the fuel weight. This is because, on the one hand, the TF configuration effectively reduces the weight of the wing, fuselage, landing gear, etc., and on the other hand, it is assumed that this next-generation TF aircraft will adopt advanced materials and structure concepts.

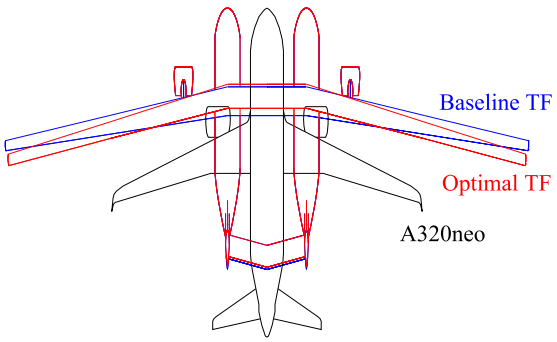

Fig. 23. Geometric comparison.

6. Comparative study of the TF configuration

A comparative study of the TF aircraft and a conventional aircraft with novel airframe technologies was conducted for the TF configuration characteristics investigation. Karpuk et al. [28] researched the influence of novel technologies, including the HLFC, active load alleviation, boundary layer ingestion, and new materials and structures, for a medium-range passenger aircraft with the conventional configuration (tube-and-wing), named SE2A medium-

Table 13
Comparison of key aircraft characteristics.

Parameter	Optimal TF (1#)	Baseline TF (2#)	A320neo (3#) [42]	Relative change (1 wrt 2), %	Relative change (1 wrt 3), %	Relative change (2 wrt 3), %
M_f, kg	10388.0	13041.0	14700.0	−20.34	−29.33	−11.29
M_{TO}, kg	52459.0	56510.0	79000.0	−7.17	−33.60	−28.47
OEW, kg	27850.0	29249.0	44300.0	−4.78	−37.13	−33.98

Table 14
Comparison of the TF configuration and the conventional configuration.

Parameter	Medium-range TF aircraft	SE2A medium-range backward-swept	A320neo [42]
M_f, kg	10388.0	11462.0	14700.0
M_{TO}, kg	52459.0	72970.0	79000.0
OEW, kg	27850.0	42259.0	44300.0

range backward-swept, which was selected for the comparative study in this paper. It should be noted that the SE2A medium-range backward-swept aircraft was designed for the timeframe 2050, so some novel technology impact assumptions were more aggressive than those in this paper. Therefore, to be fair, the novel technology impact assumptions, including laminar flow range and load factors, were modified to be consistent with this work, and the SE2A medium-range backward-swept aircraft was resized corresponding to these modifications. The comparison is given in Table 14.

Since the top-level requirements of the medium-range TF aircraft and the SE2A medium-range backward-swept aircraft, such as passenger capacity and range, are the same as the reference A320 aircraft, the performance difference between the two aircraft is mainly reflected in the fuel weight. The fuel weight and the maximum takeoff weight of the medium-range TF aircraft are 9.37% and 28.11% smaller than those of the SE2A medium-range backward-swept aircraft, which is mainly due to the TF aircraft's lighter empty weight. The significant difference between the empty weights of the two aircraft is mainly due to the lighter wing mass and fuselage mass of the TF aircraft compared to the conventional aircraft, which is because the TF aircraft's better wing spanwise load distribution and the smaller individual fuselage size. Besides, it is worth noting that since the SE2A medium-range backward-swept aircraft was designed with the propulsive fuselage concept (assumed 5% specific fuel consumption reduction due to the boundary-layer ingestion effect in Ref. [28]), the advantages of the TF aircraft over the SE2A medium-range backward-swept aircraft would be a little better than the comparison results in Table 14. In general, both aircraft with novel airframe technologies have significant performance improvements over the reference A320 aircraft.

7. Conclusion

This work addressed the problem of designing and optimizing a TF passenger aircraft. The scope was to investigate the potentials of combining novel airframe technologies with TF configuration on increasing fuel efficiency of passenger aircraft. Several methods and tools were improved and integrated into the design and analysis framework. A medium-range TF transport aircraft was designed, and the design space exploration was performed to investigate the characteristics of the TF aircraft. Based on the design and analysis framework, a GA-based MDO framework for TF aircraft was developed and used to optimize the TF aircraft configuration.

A medium-range TF transport aircraft case study demonstrated the established TF aircraft design and analysis framework. This demonstration case illustrated the design considerations of TF aircraft, especially the method and process of fuselage sizing and interior arrangement. With the same top-level requirements and mission profile, the TF aircraft consumes 29.33% less fuel than A320neo, and the OEW of the TF aircraft is 37.13% lighter, which is mainly due to the weight reduction in the wing, fuselage, and landing gear of TF configuration. A comparative study showed that the medium-range TF aircraft is more fuel-efficient than a conventional aircraft with the same novel airframe technologies, with a 9.37% lighter fuel weight.

The design space exploration of the single-parameter and the multi-parameter combination was addressed. Results indicated that the influence of each technology on the performance of the TF aircraft is different, and the HLFC technology has the most significant impact. If an advanced HLFC technology that can maintain 80% of the wing laminar flow area can be realized, the fuel weight of the TF aircraft is expected to be reduced by 42.06% compared with that without HLFC technology. The results of single-parameter sensitivity analysis showed that some parameters of the initial design were not optimal. Besides, the results of multi-parameter sensitivity analysis showed that the design parameters of TF aircraft have coupling effects, which indicates it is necessary to use MDO to find the optimal configuration of the TF aircraft.

A surrogate-based MDO framework was developed and used for the optimization of the TF aircraft. Results showed a significant improvement in fuel efficiency, up to a 20.34% decrease in fuel weight, and an MTOW reduction of 7.1%, and an OEW reduction of 4.78%.

This work preliminarily demonstrated the prospect of adopting TF configuration for the next-generation transport aircraft. Avenues for future work include the development of a dynamic aeroelastic analysis method for the conceptual and optimal design of ultra-high aspect ratio wings and the establishment and integration of aerostructural optimization method into MDO, making the MDO framework more comprehensive for TF aircraft design optimization. Furthermore, this study focused on the medium-range mission, and future research will study the benefits and performance of TF configuration in short- and long-range missions.

Declaration of competing interest

The authors declare that they have no known competing financial interests or personal relationships that could have appeared to influence the work reported in this paper.

Acknowledgements

This project has received funding from the Clean Sky 2 Joint Undertaking (JU) under grant agreement No. 883670. The JU receives support from the European Union's Horizon 2020 research and innovation programme and the Clean Sky 2 JU members other than the Union.

References

[1] A.R. Gnadt, R.L. Speth, J.S. Sabnis, S.R. Barrett, Technical and environmental assessment of all-electric 180-passenger commercial aircraft, Prog. Aerosp. Sci. 105 (2019) 1–30, https://doi.org/10.1016/j.paerosci.2018.11.002.
[2] Flightpath 2050-Europe's Vision for Aviation: Advisory Council for Aeronautics Research in Europe, European Commission, Brussels, Belgium, 2011.
[3] C. Pornet, A.T. Isikveren, Conceptual design of hybrid-electric transport aircraft, Prog. Aerosp. Sci. 79 (2015) 114–135, https://doi.org/10.1016/j.paerosci.2015.09.002.

[4] N.A. Harrison, G.M. Gatlin, S.A. Viken, M. Beyar, E.D. Dickey, K. Hoffman, E.Y. Reichenbach, Development of an efficient M = 0.80 transonic truss-braced wing aircraft, in: AIAA Scitech 2020 Forum, January 2020.
[5] T.R. Brooks, B.D. Smith, Aerostructural design optimization of the D8 aircraft using active aeroelastic tailoring, in: AIAA Scitech 2020 Forum, January 2020.
[6] P. Horst, A. Elham, R. Radespiel, Reduction of aircraft drag, loads and mass for energy transition in aeronautics, in: DLRK 2020, September 2020.
[7] N. Beck, T. Landa, A. Seitz, L. Boermans, Y. Liu, R. Radespiel, Drag reduction by laminar flow control, Energies 11 (1) (2018) 252, https://doi.org/10.3390/en11010252.
[8] Y.S. Meng, L. Yan, W. Huang, T.T. Zhang, Detailed parametric investigation and optimization of a composite wing with high aspect ratio, Int. J. Aerosp. Eng. 2019 (2019), https://doi.org/10.1155/2019/3684015.
[9] S. Chiesa, M. Di Sciuva, P. Maggiore, The double-fuselage layout: a preliminary case study of a possible way of reducing the development costs for new high-capacity aircraft, Proc. Inst. Mech. Eng., G J. Aerosp. Eng. 214 (2) (2000) 85–95, https://doi.org/10.1243/0954410001531836.
[10] M.M. Opgenoord, M. Drela, K.E. Willcox, Influence of transonic flutter on the conceptual design of next-generation transport aircraft, AIAA J. 57 (5) (2019) 1973–1987, https://doi.org/10.2514/1.J057302.
[11] T. Jong, R. Slingerland, Analysis of the twin-fuselage configuration and its H-cabin derivative, in: AIAA's 3rd Annual Aviation Technology, Integration, and Operations, November 2003.
[12] Y.V. Vedernikov, V.E. Chepiga, V.P. Maslakov, E.A. Kuklev, V.G. Gusev, Configuration of the medium-haul twin-fuselage passenger aircraft, Int. J. Appl. Eng. Res. 12 (4) (2017) 414–421.
[13] E. Torenbeek, Advanced Aircraft Design: Conceptual Design, Analysis and Optimization of Subsonic Civil Airplanes, John Wiley and Sons Ltd, West Sussex, 2013.
[14] J. Moore, D. Maddalon, Multibody transport concept, in: 2nd International Very Large Vehicles Conference, May 1982.
[15] S. Corda, C. Longo, Z. Krevor, Stratolaunch air-launched hypersonic testbed, in: 22nd AIAA International Space Planes and Hypersonics Systems and Technologies Conference, September 2018.
[16] M. Guerster, E.F. Crawley, Dominant suborbital space tourism architectures, J. Spacecr. Rockets 56 (5) (2019) 1580–1592, https://doi.org/10.2514/1.A34385.
[17] J.W. Langelaan, A. Chakrabarty, A. Deng, K. Miles, V. Plevnik, J. Tomazic, T. Tomazic, G. Veble, Green flight challenge: aircraft design and flight planning for extreme fuel efficiency, J. Aircr. 50 (3) (2013) 832–846, https://doi.org/10.2514/1.C032022.
[18] J. Kallo, DLR Leads HY4 project for four-seater fuel cell aircraft, Fuel Cells Bull. 2015 (11) (2015) 13, https://doi.org/10.1016/S1464-2859(15)30362-X.
[19] Y. Ma, W. Zhang, Y. Zhang, X. Zhang, Y. Zhong, Sizing method and sensitivity analysis for distributed electric propulsion aircraft, J. Aircr. 57 (4) (2020) 730–741, https://doi.org/10.2514/1.C035581.
[20] C. Carithers, C. Montalvo, Experimental control of two connected fixed wing aircraft, Aerospace 5 (4) (2018) 113, https://doi.org/10.3390/aerospace5040113.
[21] X. Gao, Z. Hou, Z. Guo, X. Chen, Design and performance test of a twin fuselage configuration solar-powered UAV, in: 29th Congress of the International Council of the Aeronautical Sciences, St. Petersburg, September 2014.
[22] W.D. Grantham, P.L. Deal, G.L. Keyser Jr., P.M. Smith, Simulator study of flight characteristics of a large twin-fuselage cargo transport airplane during approach and landing, NASA Technical Paper 2183, 1983.
[23] N. Weingarten, An In-Flight Investigation of a Twin Fuselage Configuration in Approach and Landing, NASA-CR-172366, National Aeronautics and Space Administration, Langley Research Center, 1985, 19850005492.
[24] S.V. Udin, W.J. Anderson, Wing mass formula for twin fuselage aircraft, J. Aircr. 29 (5) (1992) 907–914, https://doi.org/10.2514/3.46261.
[25] V.I. Chernousov, A.A. Krutov, E.A. Pigusov, Study on a twin-fuselage transport airplane model in a low speed wind tunnel, IOP Conf. Ser. Mater. Sci. Eng. 1024 (1) (2021) 012035, https://doi.org/10.1088/1757-899X/1024/1/012035.
[26] K. Risse, E. Stumpf, Conceptual aircraft design with hybrid laminar flow control, CEAS Aeronaut. J. 5 (3) (2014) 333–343, https://doi.org/10.1007/s13272-014-0111-6.
[27] C.C. Rossow, H. Von Geyr, M. Hepperle, The 1g-wing, visionary concept or naive solution?, DLR-IB-AS-BS-2016-121, 2016.
[28] S. Karpuk, A. Elham, Conceptual design trade study for an energy-efficient mid-range aircraft with novel technologies, in: AIAA Scitech 2021 Forum, January 2021.
[29] T.R. Brooks, J.R. Martins, G.J. Kennedy, High-fidelity aerostructural optimization of tow-steered composite wings, J. Fluids Struct. 88 (2019) 122–147, https://doi.org/10.1016/j.jfluidstructs.2019.04.005.
[30] A. De Marco, M. Di Stasio, P. Della Vecchia, V. Trifari, F. Nicolosi, Automatic modeling of aircraft external geometries for preliminary design workflows, Aerosp. Sci. Technol. 98 (2020) 105667, https://doi.org/10.1016/j.ast.2019.105667.
[31] T.W. Lukaczyk, A.D. Wendorff, M. Colonno, T.D. Economon, J.J. Alonso, T.H. Orra, C. Ilario, SUAVE: an open-source environment for multi-fidelity conceptual vehicle design, in: 33rd AIAA Applied Aerodynamics Conference, June 2015.
[32] J.W. Moore, E.P. Craven, B.T. Farmer, J.F. Honrath, R.E. Stephens, C.E. Bronson Jr., R.T. Meyer, J.H. Hogue, Multibody Aircraft Study, vol. I, NASA-CR-165829-VOL-1, 1982.
[33] O. Gur, M. Bhatia, W.H. Mason, J.A. Schetz, R.K. Kapania, T. Nam, Development of a framework for truss-braced wing conceptual MDO, Struct. Multidiscip. Optim. 44 (2) (2011) 277–298, https://doi.org/10.1007/s00158-010-0612-9.
[34] D.P. Wells, B.L. Horvath, L.A. McCullers, The flight optimization system weights estimation method, NASA/TM-2017-219627/Volume I, 2017.
[35] J.J. Berton, D.L. Huff, K. Geiselhart, J. Seidel, Supersonic technology concept aeroplanes for environmental studies, in: AIAA Scitech 2020 Forum, January 2020.
[36] S.A. Andrews, R.E. Perez, Comparison of box-wing and conventional aircraft mission performance using multidisciplinary analysis and optimization, Aerosp. Sci. Technol. 79 (2018) 336–351, https://doi.org/10.1016/j.ast.2018.05.060.
[37] Certification specifications and acceptable means of compliance for large aeroplanes CS-25, https://www.easa.europa.eu/document-library/certification-specifications/cs-25-amendment-25, June 2020.
[38] D. Raymer, Aircraft Design: A Conceptual Approach, 6th edition, AIAA Education Series, American Institute of Aeronautics and Astronautics, Washington, DC, 2018.
[39] E. Torenbeek, Synthesis of Subsonic Airplane Design, Springer, Netherlands, 1982.
[40] M.K. Bradley, C.K. Droney, T.J. Allen, Subsonic ultra green aircraft research: phase II – volume I – truss braced wing design exploration, NASA/CR–2015-218704/Volume I, 2015.
[41] S. Karpuk, Y. Liu, A. Elham, Multi-fidelity design optimization of a long-range blended wing body aircraft with new airframe technologies, Aerospace 7 (7) (2020) 87, https://doi.org/10.3390/aerospace7070087.
[42] Airbus S.A.S., A320 aircraft characteristics airport and maintenance planning, Issue: 30 September 1985, Rev: 1 April 2020.
[43] E.M. Greitzer, P.A. Bonnefoy, E. de la Rosa Blanco, C.S. Dorbian, M. Drela, D.K. Hall, R.J. Hansman, J.I. Hileman, R.H. Liebeck, J. Lovergren, P. Mody, J.A. Pertuze, S. Sato, Z.S. Spakovsky, C.S. Tan, J.S. Hollman, J.E. Duda, N. Fitzgerald, J. Houghton, J.L. Kerrebrock, G.F. Kiwada, D. Kordonowy, J.C. Parrish, J. Tylko, E.A. Wen, W.K. Lord, N 3 aircraft concept designs and trade studies final report, NASA CR-2010-216794/VOL2, 2010.
[44] M. Niță, D. Scholz, From preliminary aircraft cabin design to cabin optimization-part II, in: Deutscher Luft- und Raumfahrtkongress DLRK 2010, 2010.
[45] A. Elham, M.J.L. van Tooren, Effect of wing-box structure on the optimum wing outer shape, Aeronaut. J. 118 (2014) 1–30, https://doi.org/10.1017/S0001924000008903.
[46] Y. He, J. Sun, P. Song, X. Wang, A.S. Usmani, Preference-driven kriging-based multiobjective optimization method with a novel multipoint infill criterion and application to airfoil shape design, Aerosp. Sci. Technol. 96 (2020) 105555, https://doi.org/10.1016/j.ast.2019.105555.
[47] S. Lophaven, H. Nielsen, J. Sondergaard, Aspects of the Matlab toolbox DACE, Technical University of Denmark, Tech. Rept. IMMREP-2002-13, August 2002.
[48] M. Nemati, A. Jahangirian, Robust aerodynamic morphing shape optimization for high-lift missions, Aerosp. Sci. Technol. 103 (2020) 105897, https://doi.org/10.1016/j.ast.2020.105897.
[49] O. Gur, M. Bhatia, J.A. Schetz, W.H. Mason, R.K. Kapania, D.N. Mavris, Design optimization of a truss-braced-wing transonic transport aircraft, J. Aircr. 47 (6) (2010) 1907–1917, https://doi.org/10.2514/1.47546.